



# Classification of Pupil Turbidity Based On Convolutional Neural Network (CNN) As An Early Detection of Cataract Step Using A Smartphone

Dewi Mutiara Sari, Riyanto Sigit, Dias Agata, And Muhammad Firdaus Maulana

Department of Informatics and Computer Engineering Politeknik Elektronika Negeri Surabaya  
Indonesia

dewi.mutiara@pens.ac.id, riyanto@pens.ac.id  
diasagata@pens.ac.id, firdaus452maulana@gmail.com

**Abstract:** Cataracts are the number one cause of blindness in the world as well as in Indonesia according to the World Health Organization (WHO). The high cases of cataracts in Indonesia are not matched by adequate health facilities. The cataract surgery rate in Indonesia is still below the ideal cataract surgery rate. Examination using a slit lamp is carried out by professionals and special equipment, so it is relatively expensive. Prevention of cataracts can be conducted by an early detection of cataracts. This study aims to detect cataracts at an early stage by using data on the classification of pupil turbidity (turbid and normal). There are two main steps in this study, the first is iris detection using a Single Shot Multibox Detector (SSD) and then followed by pupil turbidity classification using a Convolutional Neural Network (CNN) with the MobileNet architectural model. The accuracy achieved by the system in classifying pupil turbidity is 83.3% using a dataset of 160 images of normal and cataract eyes.

**Keywords :** Pupil Turbidity; Iris Detection; Object Detection; Early Detction of Catarct.

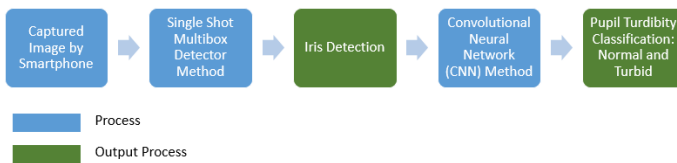
## I. INTRODUCTION

Cataracts are the most common cause of blindness in the world [1,2,3]. In fact, there are more cataract cases worldwide than all other serious eye diseases such as glaucoma, macular degeneration, and diabetic retinopathy combined. Around 2,000 cases of blindness or 2 percent in Indonesia, around 50 percent are caused by cataracts. Recently, the blindness rate has increased to 3 percent and cataracts have increased to 81 percent [4]. In 2018, 1.5 percent per two million population are cataract sufferers and every year 240 thousand people are at risk of becoming blind [1]. M. Siddik, Chair of the Indonesian Ophthalmologist Association (PERDAMI), said that ideally the cataract surgery rate would be 80 percent. Meanwhile in Indonesia it has only reached 45 percent (liputan6.com, 2019). The number of health facilities in Indonesia did not meet the enormous cases of the national blindness. Early detection of cataracts is conventionally carried out using a Slit-Lamp by an ophthalmologist. Slit-Lamp is a medical device that is able to see the state of the eye with beam lighting. The examination continued with the doctor's analysis based on the image results from the Slit-Lamp examination. Insufficient numbers of doctors in an area compared to other regions also makes health service facilities inaccessible to everyone equally.

Cataracts can be detected in the pupil area when the eye is examined externally. If the cloudy area in the pupil of the eye is relatively small then the cataract is considered at an

early stage, but if the cloudy area in the pupil nearly or fully covers the lens, then the cataract is considered at an advanced stage [2]. Blindness that occurs in people with cataracts occurs gradually without pain over a long period of time. The symptom which occurs without pain is that causes many sufferers to not realize that they already have cataracts, and some even think that they are just nearsighted or farsighted [5]. Cataracts have symptoms that vary according to the type of cataract experienced, including glare when looking at a light source, mild to severe pain, retinal bleeding [6]. There has been research conducted regarding cataract detection. Sigit R., et al, carried out a machine learning-based cataract classification but the input images were images from Slit-lamp and desktop-based examinations [1]. Then research for early detection of cataracts has also been carried out by Triyana, E., et al, using the Smartphone-based Single Layer Perceptron method but the input image was still using Slit-lamp images [7].

Based on this background, this research created a system for pupil turbidity based on Convolutional Neural Network (CNN) as an early detection of cataract using a Smartphone. The system diagram of this study is illustrated in Fig 1.



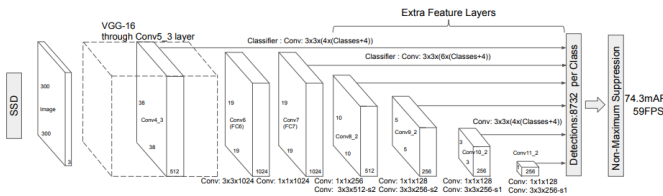
**Fig 1.** The Pipeline System of Pupil Turbidity Classification

**II. METHOD**

This section discussed into 2 parts: Iris detection by using Single Shot Multibox Detector (SSD) Method and pupil turbidity classification by using Convolutional Neural Network (CNN) Method.

**A. Iris Detection**

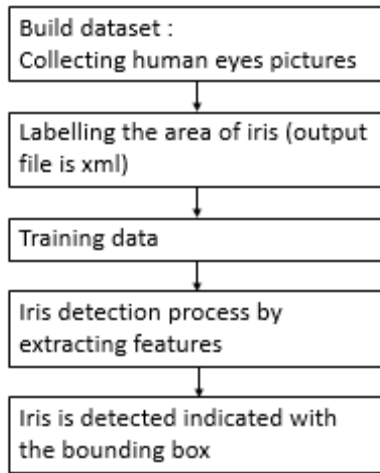
For iris detection, the method used in this research is Single Shot Multibox Detector (SSD). The architecture model of SSD is described in Fig 2.



**Fig 2.** Architecture Model of Single Shot Multibox Detector (SSD) [9]

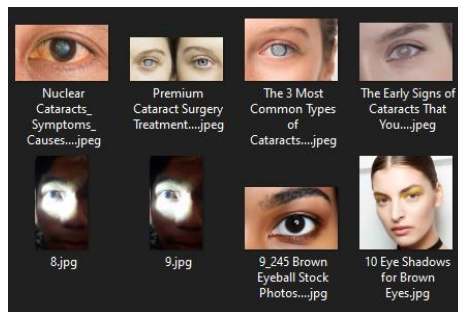
Based on Fig 2, the basic network used is VGG-16 with the input image size is 3000 x 300. There are some additional features that are embedded to the network, they are: aspect ratios and default boxes, convolutional predictors, and multi-scale feature maps. Both convolutional predictors and multi-scale feature maps are used for the detection. Then at the end of the architecture, there is a non-maximum suppression part as the last

step of the final detection [8] [9]. In general, the process of iris detection is summarized in Fig 3.



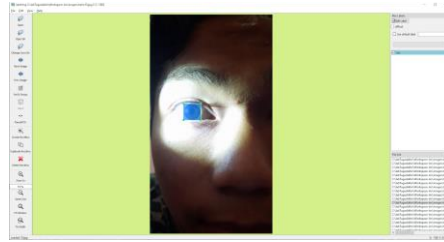
**Fig 3.** The Process of Iris Detection

The input for this process is streaming images from a smartphone camera to detect the iris area. This stage is carried out to ensure that the image taken is the iris of human's eye. The iris area detection process uses a Single Shot Multibox Detector (SSD) and MobileNet SSD as cross-trained model. Before doing the eye detection on a smartphone, the first step is to do data training to make a model of the SSD. This process begins with collecting images of the human eye to be used as a dataset. Fig 4 shows image samples suitable for dataset.



**Fig 4.** Sample of Eyes Dataset

The next step is to mark the iris area which will be used as training data and will generate an xml file. Fig. 5 shows the process of marking the iris area using labeling.



**Fig 5.** Labelling Process of Eye Area

The next step is data training using the pre-trained MobileNet SSD model as the basic model during data training. The training process is run through the command prompt (CMD) with commands according to the procedures in the training data program. The SSD model contains layers that apply the CNN method in recognizing images that enter the created model. Fig 6 shows an example of the data training process.

```
learning_rate : 0.5333205]
INFO:tensorflow:Step 700 per-step time 0.537s
I1229 17:16:49.281237 35892 model_lib_v2.py:705] Step 700 per-step time 0.537s
INFO:tensorflow:{"Loss/classification_loss": 0.8583389,
'Loss/localization_loss': 0.55271775,
'Loss/regularization_loss': 22.190475,
'Loss/total_loss': 23.601532,
'learning_rate': 0.5999999}
I1229 17:16:49.284334 35892 model_lib_v2.py:708] {"Loss/classification_loss": 0.8583389,
'Loss/localization_loss': 0.55271775,
'Loss/regularization_loss': 22.190475,
'Loss/total_loss': 23.601532,
'learning_rate': 0.5999999}
INFO:tensorflow:Step 800 per-step time 0.534s
I1229 17:17:42.392236 35892 model_lib_v2.py:705] Step 800 per-step time 0.534s
INFO:tensorflow:{"Loss/classification_loss": 1.4142104,
'Loss/localization_loss': 0.5245542,
'Loss/regularization_loss': 21.144245,
'Loss/total_loss': 23.08301,
'learning_rate': 0.6666603}
```

**Fig 6.** Data Training Process

The result of the xml file contains values in matrix form that can be used for direct eye area detection. Detection is carried out using a Single Shot Multibox Detector (SSD). The model that will be formed will have layers in which it is used to break down the features of the image. Fig. 7 is an experiment with the detection of the iris area on an Android smartphone.



**Fig 7.** Eye Area Detection Using Android Smartphone

Fig 7 shows that after the system detects the eye area using the SSD model, the system will create a bounding box in the area around the eye. The bounding box will be used as cropping. Algorithm 3.3 is used to process images from the camera to get the eye area. The architecture of the detection model is presented in TABLE I. The figure displays several layers consisting of layers from the MobileNet model and in the last part there is an additional feature layer which is a part of the SSD layer.

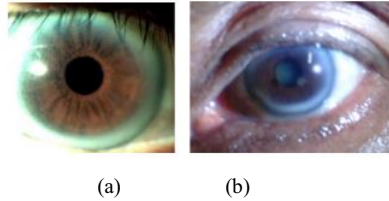
**TABLE I.** ARCHITECTURE MODEL OF IRIS DETECTION

| Type                     | Filter Shape                | Input Size   |
|--------------------------|-----------------------------|--------------|
| Conv2D                   | 32×3×3×3                    | 1×300×300×3  |
| DepthwiseConv2D          | 1×3×3×32 dw                 | 1×150×150×32 |
| Conv2D                   | 64×1×1×32                   | 1×150×150×32 |
| DepthwiseConv2D          | 1×3×3×64 dw                 | 1×150×150×64 |
| Conv2D                   | 128×1×1×64                  | 1×75×75×64   |
| DepthwiseConv2D          | 1×3×3×128 dw                | 1×75×75×128  |
| Conv2D                   | 128×1×1×128                 | 1×75×75×128  |
| DepthwiseConv2D          | 1×3×3×128 dw                | 1×75×75×128  |
| Conv2D                   | 256×1×1×128                 | 1×38×38×128  |
| DepthwiseConv2D          | 1×3×3×256 dw                | 1×38×38×256  |
| Conv2D                   | 256×1×1×256                 | 1×38×38×256  |
| DepthwiseConv2D          | 1×3×3×256 dw                | 1×38×38×256  |
| Conv2D                   | 512×1×1×256                 | 1×19×19×256  |
| 5x Conv2DDepthwiseConv2D | 1×3×3×512 dw<br>512×1×1×512 | 1×19×19×512  |
| DepthwiseConv2D          | 1×3×3×512                   | 1×19×19×512  |
| Conv2D                   | 1024×1×1×512                | 1×10×10×512  |
| DepthwiseConv2D          | 1×3×3×1024                  | 1×10×10×1024 |
| Conv2D                   | 1024×1×1×1024               | 1×10×10×1024 |
| Conv2D                   | 256×1×1×1024                | 1×10×10×1024 |
| Conv2D                   | 512×3×3×256                 | 1×10×10×256  |
| Conv2D                   | 128×1×1×512                 | 1×5×5×512    |
| Conv2D                   | 256×3×3×128                 | 1×5×5×128    |
| Conv2D                   | 128×1×1×256                 | 1×3×3×256    |
| Conv2D                   | 256×3×3×128                 | 1×3×3×128    |
| Conv2D                   | 64×1×1×256                  | 1×2×2×256    |
| Conv2D                   | 128×3×3×64                  | 1×2×2×64     |

TABLE I displays the type column which contains the type of CNN layer used in the model, and the filter shape column contains the filter used to break down feature extraction on the layer. And the input size column is the size of the image that entered the layer after processing from the previous layer. In the blue table, an additional feature layer is used to classify and provides an offset relative to the original default box shape, the score of the class.

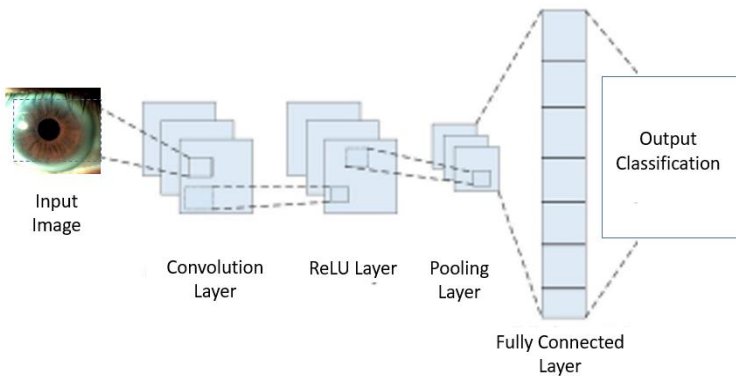
### B. Pupil Turbidity Classification

Classification was performed with a Convolutional Neural Network on the extracted iris images. In the medical field, cataracts can be distinguished physically by looking at the opacity in the pupils of the eyes. Fig 8 shows the difference between turbid and normal pupil.



**Fig 8.** (a) Normal Pupil (b) Turbid Pupil

Convolutional Neural Network (CNN) is a type of neural network commonly used in image data. CNN can be used to detect and recognize objects in an image. CNN is a technique inspired by the way humans generate visual perception. Broadly speaking, a Convolutional Neural Network (CNN) is not much different from a normal neural network. CNN consists of neurons that have weights, biases and activation functions. The convolutional layer also consists of neurons arranged in such a way as to form a filter with length and height (pixels). CNN takes advantage of the convolution process by moving a convolution kernel (filter) of a certain size to an image, the computer gets new representative information from the multiplication of the part of the image with the filter used. The architecture of CNN is divided into 2 major parts, the Feature Extraction Layer and the Fully-Connected Layer (MLP). An architectural illustration from CNN is shown in Fig 9.



**Fig 9.** Architecture of CNN

Every layer has an input  $i$  which has width ( $x$ ), height ( $x$ ), and depth ( $z$ ). Kernel Filters presents in each layer are notated as  $Kr$ , has dimensions width ( $u$ ), height ( $u$ ), and depth ( $w$ ). Remember that the dimension input layer should be bigger than the dimension of Kernel Filters. The local connection is based on the kernels sharing the similar parameters (weight  $WKr$  and bias  $BKr$ ) to generate the feature maps  $hKr$ . The size of the  $hKr$  is  $x - u - 1$ . The formulation of feature maps is described as Eq. 1,

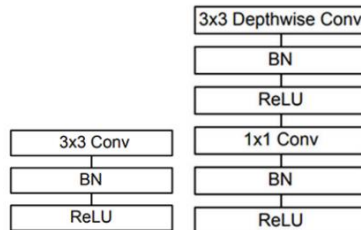
$$hKr = f(WKr * i + BKr) \tag{1}$$

Then the next step is reducing network parameters. It happens in the Pooling Layer. Each feature map conducts a down-sampling or sub-sampling process. So, it turns to the smaller feature maps. Then the Fully Connected Layer represents the CNN classifier. Every neuron inside the layer is connected to all neurons in the prior layer. The method applied here is feed-forward ANN type. In the CNN, model architecture is the important thing to be considered as it impacts the performance in the various implementations. In this case, because the device that will be used is a smartphone, the chosen model is MobileNet. MobileNet uses depth wise separable convolutions, it turns the light neuron. The architecture model of MobileNet is illustrated in Fig 10.

| Type / Stride   | Filter Shape                         | Input Size                 |
|-----------------|--------------------------------------|----------------------------|
| Conv / s2       | $3 \times 3 \times 3 \times 32$      | $224 \times 224 \times 3$  |
| Conv dw / s1    | $3 \times 3 \times 32$ dw            | $112 \times 112 \times 32$ |
| Conv / s1       | $1 \times 1 \times 32 \times 64$     | $112 \times 112 \times 32$ |
| Conv dw / s2    | $3 \times 3 \times 64$ dw            | $112 \times 112 \times 64$ |
| Conv / s1       | $1 \times 1 \times 64 \times 128$    | $56 \times 56 \times 64$   |
| Conv dw / s1    | $3 \times 3 \times 128$ dw           | $56 \times 56 \times 128$  |
| Conv / s1       | $1 \times 1 \times 128 \times 128$   | $56 \times 56 \times 128$  |
| Conv dw / s2    | $3 \times 3 \times 128$ dw           | $56 \times 56 \times 128$  |
| Conv / s1       | $1 \times 1 \times 128 \times 256$   | $28 \times 28 \times 128$  |
| Conv dw / s1    | $3 \times 3 \times 256$ dw           | $28 \times 28 \times 256$  |
| Conv / s1       | $1 \times 1 \times 256 \times 256$   | $28 \times 28 \times 256$  |
| Conv dw / s2    | $3 \times 3 \times 256$ dw           | $28 \times 28 \times 256$  |
| Conv / s1       | $1 \times 1 \times 256 \times 512$   | $14 \times 14 \times 256$  |
| 5× Conv dw / s1 | $3 \times 3 \times 512$ dw           | $14 \times 14 \times 512$  |
|                 | $1 \times 1 \times 512 \times 512$   | $14 \times 14 \times 512$  |
| Conv dw / s2    | $3 \times 3 \times 512$ dw           | $14 \times 14 \times 512$  |
| Conv / s1       | $1 \times 1 \times 512 \times 1024$  | $7 \times 7 \times 512$    |
| Conv dw / s2    | $3 \times 3 \times 1024$ dw          | $7 \times 7 \times 1024$   |
| Conv / s1       | $1 \times 1 \times 1024 \times 1024$ | $7 \times 7 \times 1024$   |
| Avg Pool / s1   | Pool $7 \times 7$                    | $7 \times 7 \times 1024$   |
| FC / s1         | $1024 \times 1000$                   | $1 \times 1 \times 1024$   |
| Softmax / s1    | Classifier                           | $1 \times 1 \times 1000$   |

**Fig 10.** Architecture Model of MobileNet

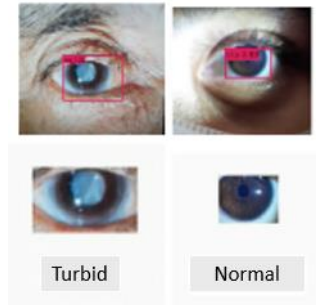
The special feature of the MobileNet architectural model compared to other architectural models is dividing the convolution into  $3 \times 3$  depth-wise conv and  $1 \times 1$  pointwise conv, as shown in Fig. 11.



**Fig 11.** (a) Standard Convolutional Layer (b) Depth-Wise Separable Convolution

In training the MobileNet model for classification, this study used 160 images of normal and cloudy eyes (cataracts). The model gains about 95% accuracy and loses about 10%.

The system classifies the image obtained from the iris detection that has been cropped. Fig. 12 shows an experiment on classifying pupillary opacities with iris image input at the iris detection stage.



**Fig 12.** Classification of Pupil Turbidity a) Turbid Pupil b) Normal Pupil

The sample training data for cloudy pupils and normal pupils in this study are shown in TABLE II.

**TABLE II.** SAMPLE OF DATA TRAINING





| No. | Training Images   | Condition |
|-----|---|-----------|
| 1   |    | Normal    |
| 2   |  | Normal    |
| 3   |  | Turbid    |
| 4   |  | Turbid    |

TABLE II shows the difference between normal eyes and cataract eyes in the pupil color of the eye. In normal eyes the pupil color tends to be black (darker), whereas in cataract eyes the pupil color tends to be white (lighter). Because in cataract eyes, there is



cloudiness in the pupil of the eye that partially or completely covers the entire lens of the eye [3].

### III. RESULT AND DISCUSSION

There are three main parts that will be discussed in this section: Accessing Smartphone Camera, Iris Detection, and Pupil Turbidity Classification. In addition, the experimental setup of this research is illustrated in Fig 13.

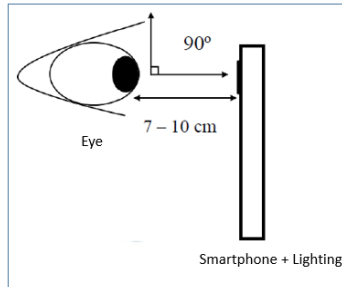


Fig 13. Experimental Setup Illustration

Based on Fig 13, the optimal distance between the camera and the eye is 7 - 10 cm with the perpendicular angle. Meanwhile for the lighting, it is conducted in the indoor room with the external lighting (not the flash of a smartphone) about 2 - 19 Lux with no shadow or reflection of the lighting. The resolution of the camera used in this research is 13 MP. Meanwhile, the detail specification of the PC device used is described in TABLE III.

TABLE III. SPECIFICATION OF PC

| No. | Description      | Specification   |
|-----|------------------|---|
| 1   | Processor        | Intel(R) Core(TM) i7-7700HQ CPU @ 2.80GHz (8 CPUs), ~2.8GHz |
| 2   | Graphic          | NVIDIA GeForce GTX 1050                                     |
| 3   | RAM              | 16384 MB  |
| 4   | Operating System | Windows 10 Home Single Language 64-bit (10.0, Build 19043)  |
| 5   | Software Build   | Android Studio  |
| 6   | Library          | OpenCV 3.4.13, TensorFlow 1.15, TFLite, Android SDK         |

The specification of smartphone used in this research is described in TABLE IV.

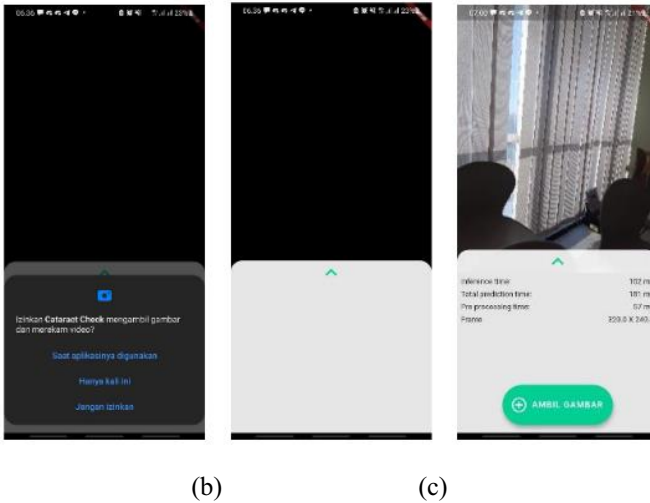
TABLE IV. SPECIFICATION OF SMARTPHONE

| No. | Description | Specification   |
|-----|-------------|---|
| 1   | Processor   | Octa-core (4x2.3 GHz Cortex-A73 & 4x1.7 GHz Cortex-A53) |

|   |                 |  |
|---|-----------------|--|
| 2 | RAM             | 6.00 GB  |
| 3 | Sistem Operasi  | Android 11, One UI 3.1                         |
| 4 | Resolusi Kamera | 48 MP, f/2.0, 26mm (wide), 1/2.0", 0.8µm, PDAF |

### A. Accessing Smartphone Camera

The System testing is carried out by running the program on an Android smartphone to check whether the application is granting permission to access the Android smartphone camera and getting real-time images from the smartphone camera. An illustration of camera access on a smartphone is shown in Fig 14.







**Fig 14.** (a) Application Asking for Accessing Smartphone Camera (b) Accessing Smartphone Camera is Rejected (c) Accessing Smartphone Camera is Accepted

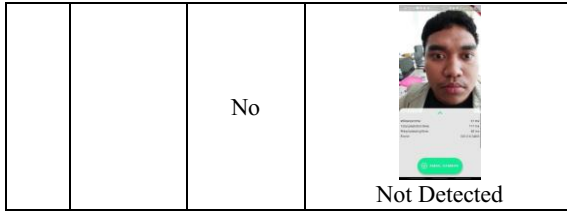
Fig 14 (a) shows an application requesting for camera access from a smartphone. If the user rejects the application's request to access the android smartphone camera, the application will not be able to get images from the camera, shown in Fig 14 (b). Fig 14 (c) shows an application given access to use the smartphone camera and obtain images via the smartphone camera.

### B. Iris Detection

This test was carried out by trying the results of training data in the form of the MobileNet SSD model which has been converted to a lite model to be able to run on Android smartphones. The iris detection stage is used to detect the eye area in images taken from Android smartphone cameras. Iris detection testing was carried out using a distance of 5, 7, 10, and 15 cm with additional light and without additional light. The test was also carried out on Android directly. The results of iris testing are summarized in TABLE V.

**TABLE V.** IRIS DETECTION RESULT

| No. | Distance | External Lighting | Iris Detection Result   |
|-----|----------|-------------------|---|
| 1   | 5 cm     | Yes               |  <p>Detected</p>       |
|     |          | No                |  <p>Not Detected</p>   |
| 2   | 7 cm     | Yes               |  <p>Detected</p>       |
|     |          | No                |  <p>Not Detected</p>   |
| 3   | 10 cm    | Yes               |  <p>Detected</p>     |
|     |          | No                |  <p>Not Detected</p> |
| 4   | 15 cm    | Yes               |  <p>Detected</p>     |



Based on the iris detection experiment in TABLE V, it is concluded that the system can detect the iris if there is external lighting.

**C. Pupil Turbidity Classification**

This test was carried out by trying the results of training data in the form of a classification model using Mobilenet which has been converted to a lite model to run on an Android smartphone. The classification stage is used to classify images of the iris that have been cropped at the iris detection stage. TABLE VI shows the Confussion Matrix which was made by testing 12 normal and cloudy eye images from the testing data. After going through a training process with a total data of around 160 images of normal eyes and cataract eyes, it produces a CNN model with a base model using MobileNet to lighten the model when running on an Android smartphone. Fig 15 shows a graph of loss and accuracy during training.



**Fig 15.** Loss Graph of Training Mode

Based on Fig 15, the graph shows a stable value in 0.1 with the beginning epoch is unstable. Table

**TABLE VI.** CONFUSION MATRIX









|                 |               |               |               |
|-----------------|---------------|---------------|---------------|
|                 |               | <b>Aktual</b> |               |
|                 |               | <b>Normal</b> | <b>Turbid</b> |
| <b>Prediksi</b> | <b>Normal</b> | 9             | 3             |
|                 | <b>Turbid</b> | 1             | 11            |

Based on TABLE VI, the system can correctly classify 12 images of normal eyes and 11 images of cloudy or cataract eyes. Table 4.6 shows that the True Positive (TP) values are 9 which in the table above is a Normal eye prediction system and these predictions are correct. Furthermore, the True Negative (TN) value is 11 data, which is a system that predicts cloudy eyes and the prediction is correct. The False Positive (FP) value is 3, and the False Negative (FN) value is 1. These two values are the opposite of the TP and TN values. By identifying these four values, it is possible to calculate the accuracy value of the image classification model of normal eyes and cloudy eyes. Using a total of 24 tested data can be calculated with Eq. (2).

$$\begin{aligned}
 \text{Accuracy} &= (TP+TN) / (TP+FP+FN+TN) \quad (2) \\
 &= (9+11) / (9+3+1+11) \\
 &= 0833 \\
 &= 0.833*100\%=83.3\%
 \end{aligned}$$

From the calculation of Eq.2, it is clear that the model has an accuracy of 83.3%. The results of the pupil turbidity classification test using data testing are summarized in TABLE VII.

**TABLE VII. RESULT OF PUPIL TURBIDITY CLASSIFICATION**

| No. | Input Picture   | Confidence Value | Classification Result | Actual Condition |
|-----|---|------------------|-----------------------|------------------|
| 1   |    | 63.15%           | Turbid                | Turbid           |
| 2   |    | 99.99%           | Turbid                | Turbid           |
| 3   |   | 99.95%           | Turbid                | Turbid           |
| 4   |  | 84.54%           | Normal                | Turbid           |
| 5   |  | 97.53%           | Normal                | Normal           |
| 6   |  | 80.98%           | Turbid                | Normal           |
| 7   |  | 72.00%           | Normal                | Normal           |
| 8   |  | 64.76%           | Normal                | Normal           |



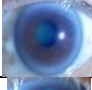
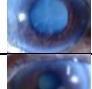

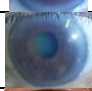

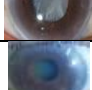
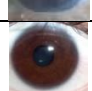


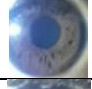


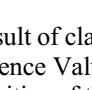
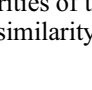
|    |   |        |        |        |
|----|---|--------|--------|--------|
| 9  |    | 90.47% | Normal | Normal |
| 10 |    | 72.27% | Turbid | Normal |
| 11 |    | 76.21% | Turbid | Turbid |
| 12 |    | 99.97% | Turbid | Turbid |
| 13 |    | 90.39% | Turbid | Turbid |
| 14 |    | 90.59% | Turbid | Turbid |
| 15 |    | 89.72% | Turbid | Turbid |
| 16 |    | 99.88% | Turbid | Turbid |
| 17 |   | 99.92% | Turbid | Turbid |
| 18 |  | 95.31% | Turbid | Turbid |
| 19 |  | 97.23% | Normal | Normal |
| 20 |  | 90.18% | Normal | Normal |
| 21 |  | 86.36% | Normal | Normal |
| 22 |  | 68.66% | Turbid | Normal |
| 23 |  | 99.45% | Normal | Normal |
| 24 |  | 95.20% | Normal | Normal |

TABLE VII is the result of classification testing using data testing. TABLE VII displays that there is a Confidence Value column which is a value that is influenced by the many variations and similarities of the class types classified. The higher the confidence value, the closer the image similarity to a class.

#### IV. CONCLUSION

Based on the results of testing and analysis that has been done, it can be concluded that the process of detecting cataracts is done by detecting the iris area first. The iris area detection process was using Single Shot Multibox Detection (SSD) and MobileNet SSD as a cross-trained model. Early classification of cataracts through the classification of pupillary opacities is carried out by using the Convolutional Neural Network (CNN) method. The system can detect cataracts from a distance of 5 to 15 cm using external lighting with a classification accuracy of 83.3%. For future work, the system will be add the expert system algorithm such that it can classify the type of cataract.

#### V. ACKNOWLEDGMENT

Thanks to Penelitian Lokal PENS for giving the funding to this research.

#### REFERENCES

- 1 Riyanto Sigit, S. M., Satmoko, M. B., & Dwi Kurnia Basuki, S. M.: (2018). Classification of Cataract Slit-lamp Image Based on Machine Learning. International Seminar on Application for Technology of Information and Communication (iSemantic), (pp. 597-602). Surabaya-East Java, Indonesia.
- 2 Tawfik, H. R., Birry, R. A., & Saad, A. A.: (2018). Early Recognition and Grading of Cataract Using a Combined Log Gabor/Discrete Wavelet Transform with ANN and SVM. International Journal of Computer and Information Engineering, 12, 1038-1043.
- 3 Liu, Y.-C., Wilkins, M., Kim, T., Malyugin, B., & Mehta, J. S.: (2017). Cataracts. Lancet, Vol. 390, 600 - 612.
- 4 Syarifah, F.: (2020, Oktober 06). Hari Penglihatan Sedunia, Kemenkes: 81 Persen Kebutaan Terjadi Akibat Katarak. Diambil kembali dari liputan6: <https://www.liputan6.com/health/read/4375562/hari-penglihatan-sedunia-kemenkes-81-persen-kebutaan-terjadi-akibat-katarak> (diakses tanggal 13 Juli 2021)
- 5 Raenida, R., & Zuhri, Z.: (2019). Sistem Pakar Diagnosis Dini Penyakit Katarak Menggunakan Metode Rule Based Reasoning. Seminar Nasional Informatika Medis (SNIMed) 2019, (pp. 52 - 58).
- 6 Astari, P.: (2018). Katarak: Klasifikasi, Tatalaksana, dan Komplikasi Operasi., (pp. 748 - 753).
- 7 Sigit, R. et al.: (2019). Cataract Detection Using Single Layer Perceptron Based on Smartphone. International Conference on Informatics and Computing Science (ICICoS).
- 8 Liu, W.: et al. SSD : Single Shot Multibox Detector. Internship Project at Google.
- 9 Alzubaidi, L. et al.: (2021). Review of Deep Learning : Concept, CNN Architectures, Challenges, Applications, Future Directions. Journal of Big Data, Springer Open.

**Open Access** This chapter is licensed under the terms of the Creative Commons Attribution-NonCommercial 4.0 International License (<http://creativecommons.org/licenses/by-nc/4.0/>), which permits any noncommercial use, sharing, adaptation, distribution and reproduction in any medium or format, as long as you give appropriate credit to the original author(s) and the source, provide a link to the Creative Commons license and indicate if changes were made.

The images or other third party material in this chapter are included in the chapter's Creative Commons license, unless indicated otherwise in a credit line to the material. If material is not included in the chapter's Creative Commons license and your intended use is not permitted by statutory regulation or exceeds the permitted use, you will need to obtain permission directly from the copyright holder.

